Performance of an Applied Field MPD Thruster*†

F. Paganucci, P. Rossetti, M. Andrenucci
Centrospazio
Via Gherardesca 5
I-56014, Pisa, Italia
+39-50-985097
f.paganucci@cpr.it
V. B. Tikhonov, V. A. Obukhov
RIAME-MAI
Volokolamskoe shosse, 4
125810, Moscow, Russia
+7-095-1580020

IEPC-01-132

The performance of a new design argon-fed, applied field MPD thruster has been experimentally investigated as a function of the mass flow rate and the intensity of the applied magnetic field. The thruster is powered by a pulse forming network, capable of delivering up to 15 kA for 2.5 ms. Electrical characteristics and thrust have been measured for 220 and 660 mg/s of argon, with and without the external magnetic field. Tests with the applied field have been carried out with a maximum induction field on the thruster axis of 40 and 80 mT. The results indicate the application of an external magnetic field can significantly increase the thruster performance, expecially at low power (up to 400 kW) and mass flow rate (220 mg/s), while at higher power and mass flow rate its contribution seems to be less important or negligible, yielding in some cases to a decay of the performance with respect to a self-field operation (660 mg/s, 40 mT, beyond 500 kW). A thrust model whose results appear in good agreement with the experimental data is also proposed. The improvement of the performance seems to strongly depend on the Hall acceleration mechanism, which, at low power, seems to be by far the dominant source for thrust generation.

Introduction

The steady increase of electric power onboard of space vehicles will allow the accomplishment of more and more missions with electric thrusters. For power ranging from 50 to 500 kW, a competitive propulsion option for primary missions (i.e. earth-orbit and interplanetary transfers) seems to be represented by applied field MPD thrusters (AFMPDTs), as demonstrated by several research efforts spent worldwide since many years [1]. The recognized main features of AFMPDTs are the high specific impulse (1000 to 5000 s), high thrust density, robustness, relative simplicity and capability, in principle, of using a large variety of propellants. These features are mostly shared with the self-field MPD thrusters, whose optimal power range is however yet higher. As a matter of fact, in self-field MPD thrusters, the main acceleration mechanism is represented by the interaction between the discharge current and the self-induced magnetic field (self-magnetic acceleration): high thrust level can be obtained only for high discharge currents (5-100 kA) and, consequently, for high powers (MWs). On the contrary, the application

* Presented as Paper IEPC-01-132 at the 27th International Electric Propulsion Conference, Pasadena, CA, 15-19 October, 2001.

of an applied magnetic field introduces new acceleration mechanisms that do not directly depend on the discharge current and thus can allow the thruster to effectively operate at lower powers. These new acceleration mechanisms are mainly two, and the weight of each in thrust generation depends on the operational conditions [2]:

- as in a SPT thruster, due to the electron drift induced by the axial component of the applied magnetic field, an azimuthal current is generated which, interacting with the radial components of the applied magnetic field, yields an axial plasma acceleration (Hall acceleration);
- the interaction between the radial component of the discharge current and the axial component of the applied magnetic field introduces a swirling motion into the plasma which, due to collisions, increase the plasma thermalization and hence the gasdynamic contribution to thrust (gasdynamic acceleration).

Other advantages in adopting an applied magnetic field are represented by an higher discharge stability and a potential reduction of electrode erosion and thus a longer lifetime of the thruster. In fact, being the same the power, the thrust and the mass flow rate, an AFMPDT will operate at a lower arc current (and higher arc voltage) than a self-field MPD thruster: the electrodes (especially the cathode) will be less stressed and thus their life prolonged.

In this context, a new AFMPDT (called "Hybrid Plasma Thruster" - HPT) has been proposed, developed and tested in the framework of a joint activity between Centrospazio and RIAME-MAI. Two almost identical prototypes have been developed and are currently under testing in each laboratory [3, 4]. In the following some of the results gathered so far on Centrospazio prototype are illustrated and analyzed.

Experimental Apparatus

The experimental apparatus HPT, shown in Fig.1, is an axisymmetric MPD thruster with an applied magnetic field. The HPT consists of a central hollow cathode (copper, 20 mm diameter, 50 mm length), through which 70-90% of a gaseous propellant is injected in the discharge chamber, and an anode, consisting of a cylinder (aluminum, 200 mm inner diameter, 180 mm length) and eight straps, made of copper, which divide a central chamber from a peripheral chamber. The straps are shaped to get their surface parallel to the local externally applied magnetic field lines. 10-30% of the propellant is injected through eight peripheral hollow electrodes (copper, 12 mm in diameter each). These electrodes can be used as auxiliary cathodes to pre-ionise the peripheral propellant by means of a secondary discharge between the cathodes and the anode. The peripheral electrodes were not activated during the tests described herein. A 70-turns coil surrounds the thruster and can be powered in order to generate a magnetic field up to 100 mT on the thruster axis.

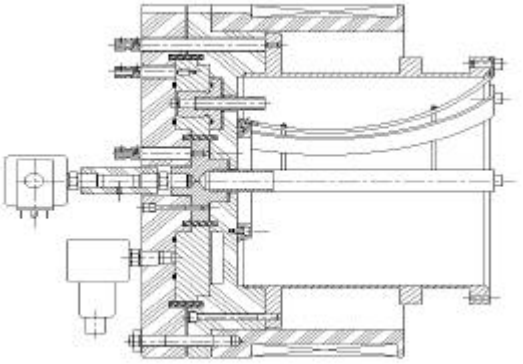

Fig. 1: Schematic drawing of the thruster assembly.

Test Equipment

The thruster is mounted on a thrust stand inside the Centrospazio IV3 vacuum chamber, capable of maintaining a back pressure before and during the pulse in the 10^{-4} mbar range (Fig.2). The electric power to the HPT is supplied by a Pulse Forming Network (PFN), configurated to supply quasi-steady current pulses 2.5 ms long. The propellant is injected by two separated gas feeding systems, one for the central cathode and the other for the peripheral cathodes, based on fast acting solenoid valves, which provide gas pulses with long plateau after few milliseconds from valve activation. The steady mass flow rate and the time between valve activation and the steady mass flow condition were obtained experimentally as described in [5]. Mass flow rate uncertainty is within 5% of the measurement. The magnetic coil is supplied by the discharge of a 10 mF capacitor bank by means of an SCR. As shown experimentally, a quasi-steady magnetic field lasting about 10 ms is obtained after 25 ms from the SCR switching on [6]. A laboratory-made digital device allows to set the sequence of the SCR and the solenoid valve activation in order to start the arc discharge when a steady condition is reached for both the applied magnetic field and the mass flow rate. The arc

ignition is obtained by closing the main circuit by switching an ignitron on. The arc current has been measured with a Hall effect current probe (LEM® LT 4000-S). To avoid anomalous discharge involving the vacuum chamber, the thruster electrodes are floating with respect to the ground and the arc voltage has been measured by measuring the potential of each electrode with respect to the ground by means of two high voltage probes (Tek 6015). The arc voltage is then obtained by subtracting the cathode voltage signal from the anode voltage signal. Fig.3 shows typical measured arc current and voltage signals.

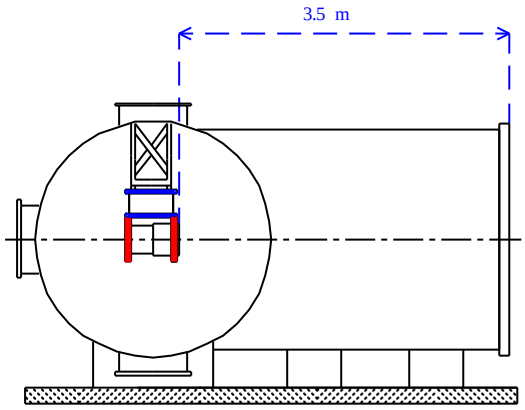

Fig.2: Thruster arrangement in the vacuum chamber.

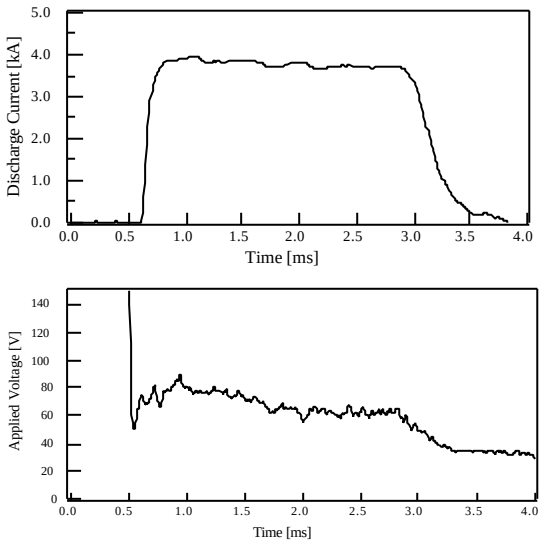

Fig. 3: Typcal arc current and voltage signals.

Applied magnetic field mapping

Fig.4 shows a mapping of the applied magnetic field. The induction field has been measured with a Hall effect probe (Honeywell® 634SS2), placed on a moving system which allows the probe to be positioned and oriented inside and in front of the thruster. The induction field has been measured with an overall accuracy of 4%. Mapping has been carried out by suppling the coil with both a DC generator and the capacitor bank. Tests have shown the magnetic field obtained during quasi-steady phase of the pulsed operation is the same as a continuous operation, provided a slightly higher current is supplied [6].

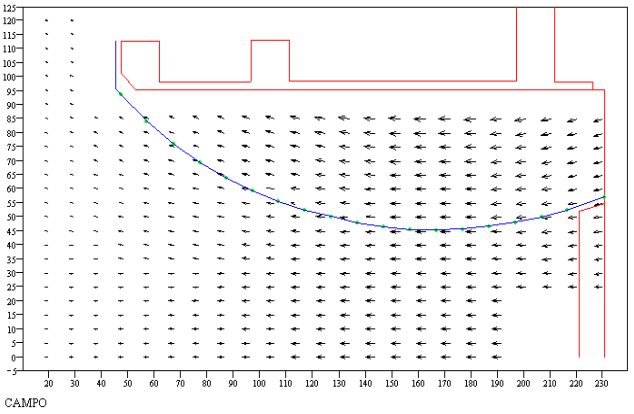

Fig. 4: Experimental mapping of the applied magnetic field.

Thrust stand and thrust measurement procedure

The thrust stand consists of two double pendulums, acting like a four–bar link, which leaves the thruster free to move only in the axial direction. The hinges at the ends of the bars consist of thin phosphor bronze straps, that, for small dispacements, act as virtual hinges with negligible disturbances to the mobility of the system. The suspension is fixed at the vacuum chamber by means of a stiff frame. The thruster is attached to the suspension by means of two supports, as illustrated in Fig.5. A proximity transducer (Bently Nevada® 7200) is used to measure the mobile mass displacement. A computerized procedure has been developed to get the thrust imput bit by knowing the mobile mass weight (about 34 kg) and measuring its motion law in a period around the shot, as shown in Fig.6. The input bits so obtained were then purged by spurious effects due to cold gas injection and the activation of the external magnetic field. These effects were previously measured by using the same procedure without the activation of the arc discharge. The method allow the net thrust impulse bit to be measured with an accuracy of about 10% of the value.

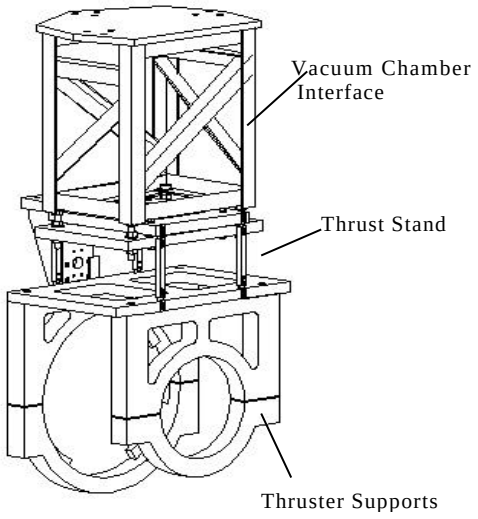

Fig. 5: Thrust stand layout.

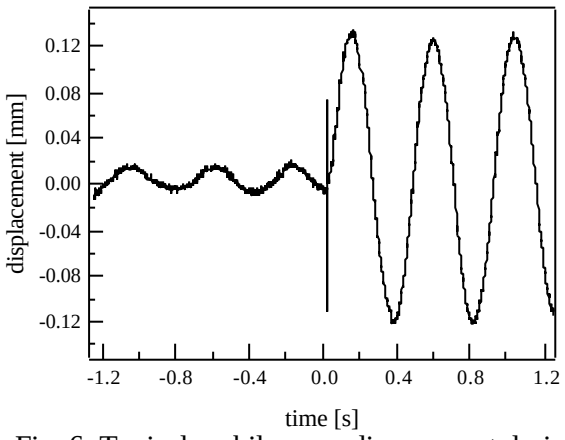

Fig. 6: Typical mobile mass dispacement during a shot.

Electrical Characteristic and Thrust Measurements

Tests were performed at 220 and 660 mg/s of argon (200 (600) mg/s injected by the central cathode, 20 (60) mg/s by the peripheral electrodes). The conditions with no applied magnetic field and with an applied field (maximum applied induction field of 40 and 80 mT on the axis) were investigated. For each shot, a current and voltage values were obtained as an average on a window 100 microseconds long taken in the middle of the pulse. Thrust is obtained by dividing the measured thrust impulse bit time the pulse duration, and thus the value represents an average thrust for each shot. Each data point in Figs.7-10 was obtained as an average of the relevant values obtained from four-five shots at the same nominal condition (i.e. PFN charging voltage). Current and voltage measurements showed a good repeatibility (the uncertatainty is withing the marker dimension). Error bars on thrust measurements include both the standard deviation and the measurement uncertainty.

Figs.7 and 8 show the electrical characteristics at the various applied field intensity for 220 and 660 mg/s of argon, respectively. As illustrated in Figs. 7 and 8, for both the mass flow rates, the same the current, the application of an external magnetic field yields an increase of the arc voltage of about 20-25 V passing from 0 to 40 mT as well as from 40 to 80 mT.

Fig.9 shows the thrust dependance on the applied magnetic field and the arc current at 220 mg/s. An increase (in the order of 1 N) has been observed for all the currents passing from 0 to 40 mT and from 40 mT to 80 mT. At 660 mg/s, thrust dependance on applied field looks more complex. For current below 5000 A, thrust increases by increasing the applied magnetic field similarly to the 220 mg/s case. For current higher than 5000 A, data relevant to 40 mT tends to merge with data obtained with a self-field operation. The same behavior seems to occur also for an applied field of 80 mT, although at higher currents (beyond 8000 A).

Experimental data analysis

The experimental data have been analyzed by means of a semi-empirical model, proposed in [7]. For a self-field operation, it assumes the thrust (T_{self}) given by:

$$T_{self} = (1.33 + \frac{1}{2A_0}) x 10^{-7} I^2$$

with:

$$A_0 = 0.833 x 10^{-7} \frac{I^2}{a\dot{m}}$$

being I the arc current, a the ion sound velocity at the thruster exit (equal to about 4500 m/s, assuming a temperature of about 3 eV) and m the mass flow rate.

For an operation with an applied magnetic field, the model considers two contributions to thrust:

$$T = T_{self} + T_{Hall}$$

where the first term is the same as in the self-field case and the second takes into account the Hall effect contribution to thrust, given by:

$$T_{Hall} = k_f I B_a D_a$$

Where k_f is an empirical coefficient, here taken equal to 0.1, as found from experiments on a lithium MPD thruster [8], B_a is the induction field on the axis at the thruster exit (equal to $0.54B_{max}$ from mapping) and D_a is the exit anode diameter.

As illustrated in Figs.11 and 12, the experimental data relevant to a self-field operation are in good agreement with the results given by the model. At 220 mg/s, as shown in Figs.11, the model yields a fairly good fitting of experimental data also for an applied field of 40 mT, while slightly underestimates thrust for 80 mT. This occurrence could be explained by a not negligible gasdynamic contribution to thrust that is neglected by the model. At 660 mg/s and 40 mT (Fig.12) the model results are in good agreement with experimental data up to 5000 A. For higher currents the model significantly overestimates the thrust. The same seems to occur also for 80 mT at current higher than 7000 A. This discrepancy could be explained by a significant plasma rarefaction in the peripheral region of the acceleration chamber, due to pinch and Hall effects occurring at high current. Since the Hall contribution to thrust almost originates in that region, a plasma rarefaction should imply a reduction of this contribution.

About the onset critical current for the various operation conditions, a general relationship which expresses a critical A_0 (A_{0cr}) as a function of the anode to cathode diameter ratio D (in this case equal to 10) can be used:

$$A_{0cr} = \frac{3.6}{D - 0.5}$$

which, for a self-field operation, yields a critical current of 2100 A for 220 mg/s and of 3700 A for 660 mg/s. Consequently, the thruster seems to have operated at currents significantly higher than the critical values given by the model.

Critical conditions for applied field operation can be obtained by the relationship [7]:

$$A_{0cr} = \frac{I_{cr} B_c (R_a - R_c) x10^{-7}}{m_0 a\dot{m}} = \frac{3.6}{D - 0.5}$$

where B_c is a sum of the self and applied magnetic fields at the cathode tip, R_a and R_c are the anode and cathode radius respectively, m_0 is the magnetic vacuum permeability. The above expression gives a critical current ranging between 1500 and 2500 A for all the conditions with the applied field. Hence, the thruster seems to have operated at super-critical condition also in these cases.

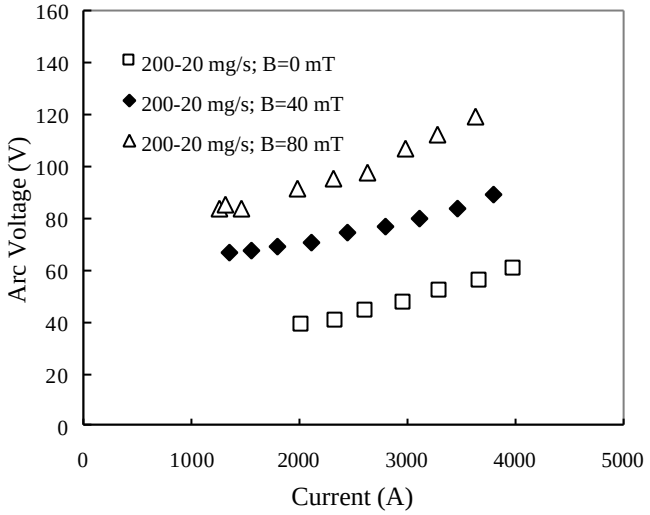

Fig.7: Electrical characteristic at 220 mg/s of argon.

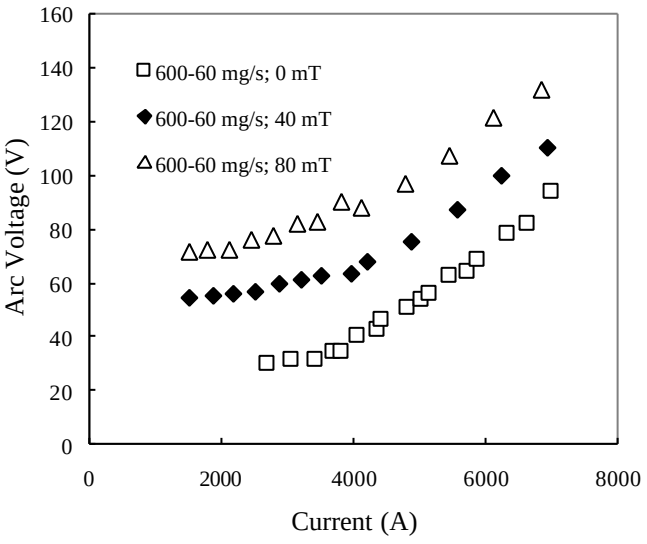

Fig.8: Electrical characteristic at 660 mg/s of argon.

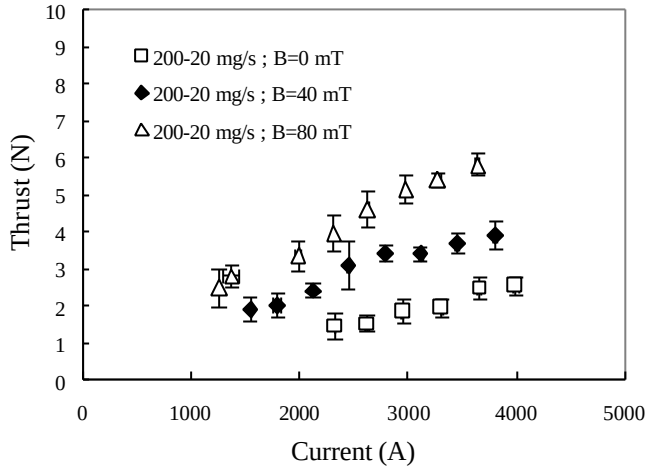

Fig.9: Thrust at 220 mg/s of argon.

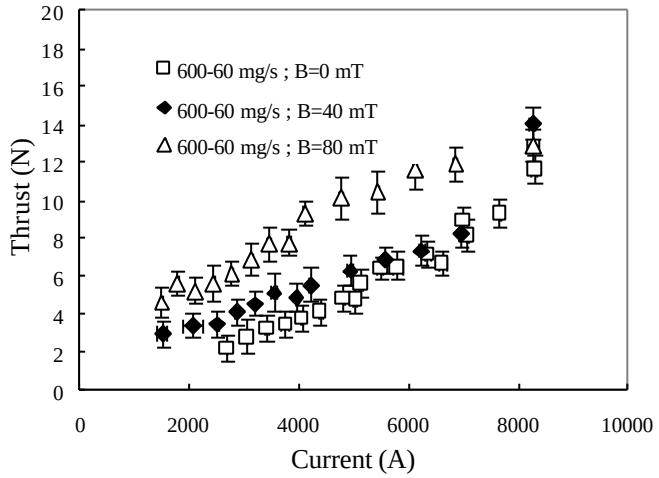

Fig.10: Thrust at 660 mg/s of argon.

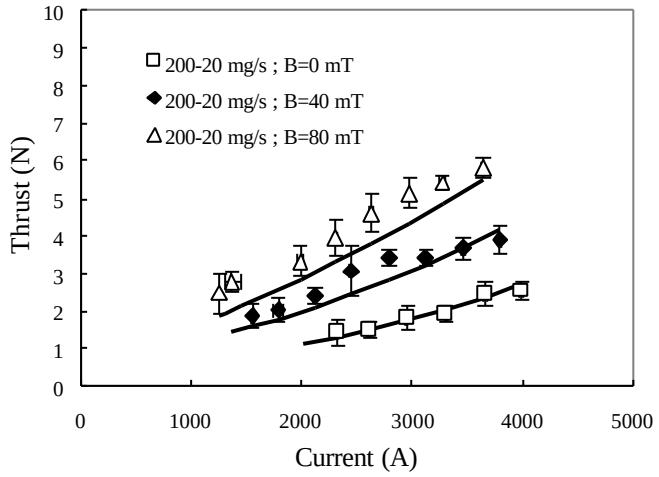

Fig.11: Comparison between experimental data (markers) and model results (lines) (argon, 220 mg/s).

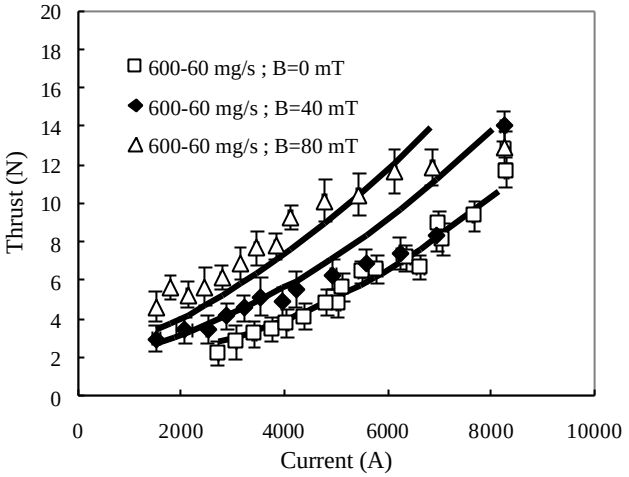

Fig.12: Comparison between experimental data (markers) and model results (lines) (argon, 660 mg/s).

Thruster Performance

Figs. 13-18 show thruster performance calculated on the basis of the experimental results. For specific impulse and thrust efficiency calculations, thrust data have been interpolated by linear (220 mg/s) and polynomial (660 mg/s) curves. The power supplied to the coil has been neglected. At 220 mg/s, within the power range investigated (from 80 to 430 kW), specific impulse and thrust efficiency steadily grow both with arc power and magnetic field. Maximum specific impulse and thrust efficiency are about 2740 s and 0.18 respectively, reached with an applied field of 80 mT and an arc power of 430 kW (Fig.13 and 14). At 660 mg/s, the same the power, specific impulse and thrust efficiency are almost the same in a self-field operation as with an applied field of 40 mT up to an arc power of about 500 kW and are lower in the latter case at higher power. Higher performance is obtained with and applied field of 80 mT. Nevertheless, thrust efficiency steadily decreases while increasing the power, reaching the same value of self-field operation at about 900 kW (Fig.16). At the same power, also the specific impulse looks to be the same as in a self-field operation (Fig.15).

Conclusions

A fully assessment of the HPT concept will need further tests to perform with the activation of the pre-ionization chamber. Nevertheless, the investigation

carried out so far allows to draw the following conclusions:

- at low power, Hall acceleration mechanism appears to be the most significant source for thrust generation with an externally applied magnetic field. For high applied field, also the gasdynamic contribution to thrust could be not negligible. As a consequence, thruster performance with an applied field, in terms of specific impulse and thrust efficiency, is significantly increased with respect to a self-field operation.
- at high power (greater than 500 kW), depending on the intensity of the applied field, Hall contribution to thrust seems to be less and less important, and the thrust appears to be almost the same as in a self-field operation. In same cases (i.e 660 mg/s, 40 mT) the applied field yields no significant performance increase, or even a decay. Pinch and Hall effects, which tend to rarefy the plasma in the external region of the acceleration chamber, are supposed to be the causes of this occurrence.
- although the thruster seems to have mostly operated at currents higher than the critical values, no significant onset effects have been observed on thruster performance.

Acknowledgements

The research has been partially supported by the Italian Space Agency (ASI). The italian authors would like to express their gratitude to Mr. Ugo Cesari and Mr. Alessio Belli for their collaboration in the framework of their Laurea thesis work carried out at Centrospazio.

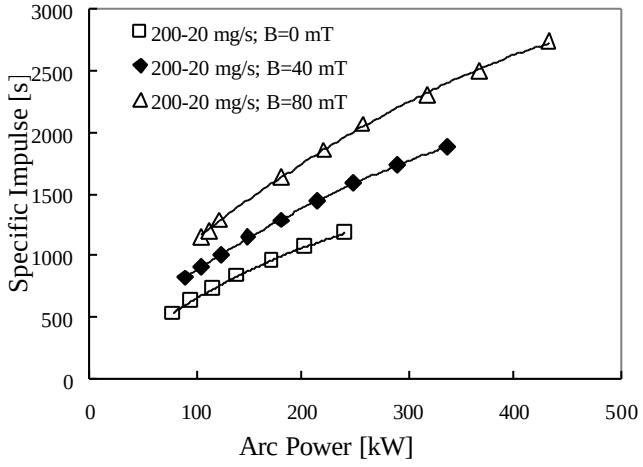

Fig.13: Specific impulse vs arc power at 220 mg/s.

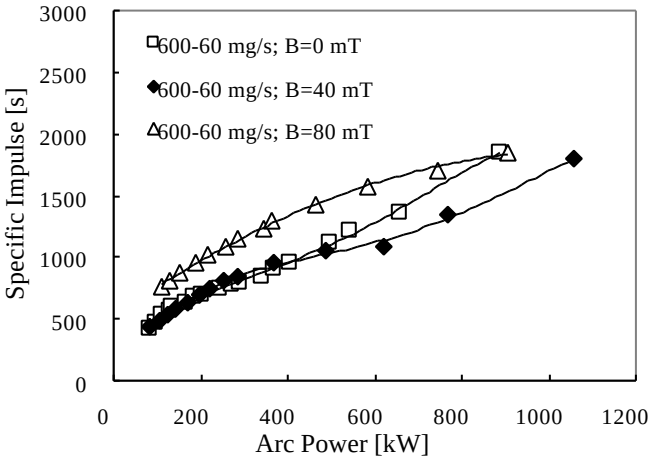

Fig.14: Specific impulse vs arc power at 660 mg/s.

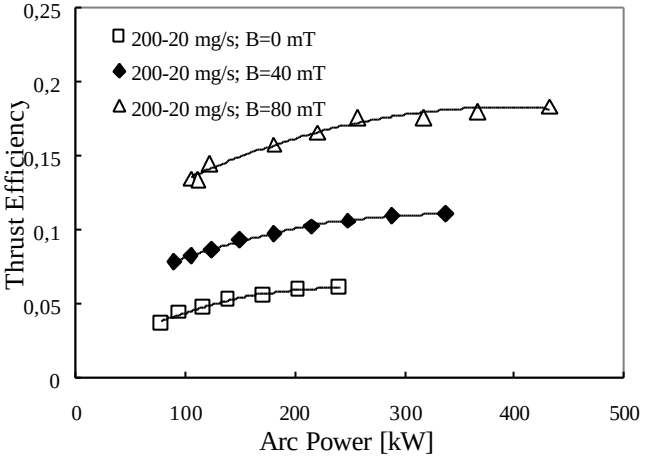

Fig.15: Thrust efficiency vs arc power at 220 mg/s.

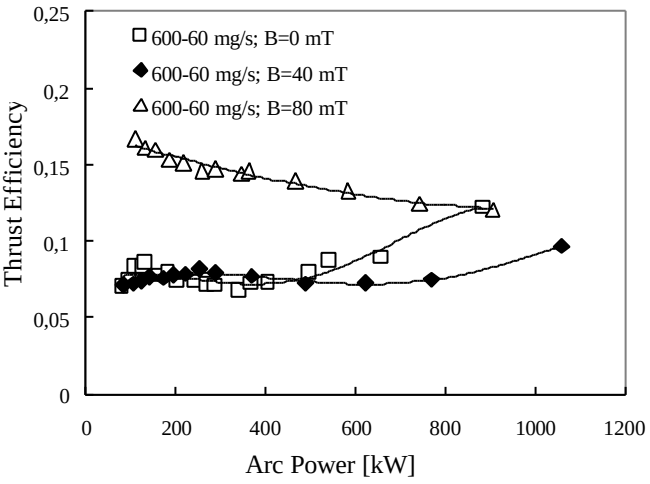

Fig.16: Thrust efficiency vs arc power at 660 mg/s.

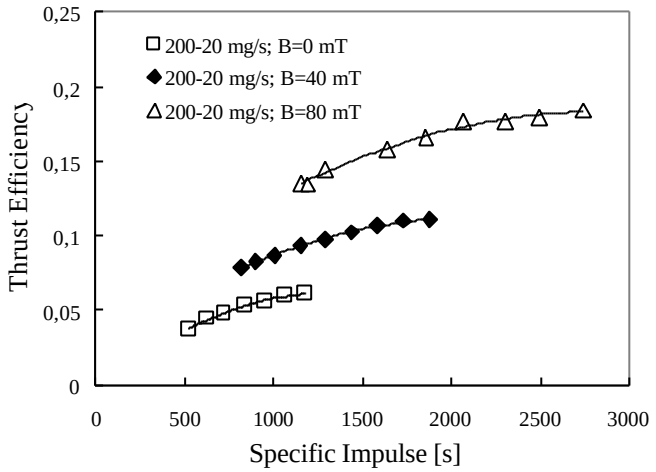

Fig.17: Thrust efficiency vs specific impulse at 220 mg/s.

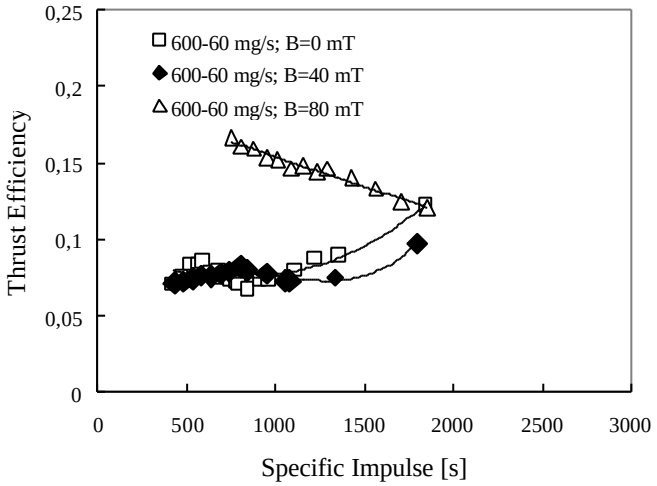

Fig.18: Thrust efficiency vs specific impulse at 660 mg/s.

References

[1] G. Krülle, M. Auweter-Kurtz, A. Sasoh, "Technology and Application Aspects of Applied Field Magnetoplasmadynamic Propulsion", Journal of Propulsion and Power, Vol 14, N. 5, Sept-Oct 1998.

[2] A. Sasoh, Y. Arakawa, "Thrust Formula for an Applied-Field MPD Thruster Derived from Energy Conservation Equation", IEPC-91-062, 22nd International Electric Propulsion Conference, Oct 1991, Viareggio, Italy.

[3] V. B. Tikhonov, *et al*, "Investigation on a New Type of MPD Thruster", paper OR21, 27th European Physical Society Conference on Controlled Fusion and Plasma Physics, Budapest, Hungary, 12-16 June 2000.

[4] V. B. Tikhonov, *et al*, "Development and Testing of a New Type of MPD Thruster", IEPC-01-123, 27th International Electric Propulsion Conference, Oct 2001, Pasadena, CA.

[5] M. Andrenucci, *et al*, "Scale Effects on the Performance of MPD Thrusters", IEPC-91-123, 22nd International Electric Propulsion Conference, Oct 1991, Viareggio, Italy.

[6] U. Cesari, "Studio e caratterizzazione del campo magnetico applicato in un propulsore MPD", Laurea Thesis, A-A 1999-2000, University of Pisa.

[7] V. B. Tikhonov, *et al*, "Research of Plasma Acceleration Processes in Self-Field and Applied Magnetic Field Thrusters", IEPC-93-76, 23rd International Electric Propulsion Conference, Sept. 1993, Seattle, WA.

[8] V. B. Tikhonov, *et al*, "Performance of a 130 kW MPD Thruster with an External Magnetic Field and Li as Propellant", IEPC 97-117, 25th International Electric Propulsion Conference, Aug. 1997, Cleveland, OH.